GSA DATA REPOSITORY 2012155

No causal link between terrestrial ecosystem change and methane release during the end-Triassic mass-extinction

Sofie Lindström [a,*], Bas van de Schootbrugge [b], Karen Dybkjær [a], Gunver Krarup Pedersen [c], Jens Fiebig [b], Lars Henrik Nielsen [a], Sylvain Richoz [d]

[a] *GEUS Geological Survey of Denmark and Greenland, Øster Voldgade 10, DK-1350 Copenhagen K, Denmark*
[b] *Institute of Geosciences, Goethe University Frankfurt, Altenhöferallee 1, D-60438, Frankfurt, Germany*
[c] *Department of Geography & Geology, Øster Voldgade 10, DK-1350 Copenhagen K, Denmark*
[d] [4]*CPSOE, Austrian Academy of Science c/o University of Graz, Heinrichstraße 26, 8020 Graz, Austria*.

**Corresponding author. E-mail address: sli@geus.dk*

GEOLOGICAL BACKGROUND

The Danish Basin is bordered towards the southwest by the Ringkøbing-Fyn High while its northeastern margin follows the NW–SE oriented Sorgenfrei-Tornquist Zone (STZ), a fundamental tectonic lineament characterized by extensive block-faulting along the southwestern margins of the Baltic Shield and transtension during the Triassic and Jurassic (Liboriussen et al., 1987; Erlström et al., 1997; Mogensen and Korstgård, 2003). During the Early Mesozoic the Danish Basin, characterized by tectonic tranquillity and a shallow marine depositional setting (Nielsen, 2003), underwent thermally controlled post-rift subsidence receiving large amounts of sediment (Liboriussen et al., 1987; Vejbæk, 1989; Erlström et al., 1997; Nielsen, 2003). The T/J-boundary succession in southern Scandinavia is overlain by younger strata in the North Sea, Denmark and the Baltic area between Sweden and Germany, and key outcrops occur only in Scania in southern Sweden. At the T/J transition southern Scandinavia was situated around 45ºN (Ziegler, 1990)(Figure DR1).

In the Danish part of the basin the Rhaetian–Hettangian succession belongs to the Gassum and Fjerritslev Formations (Pedersen, 1985; Michelsen, 1975, 1989; Nielsen, 2003). The Gassum Formation (uppermost Norian–Lower Sinemurian) varies in thickness from 50–150m in the central parts of the basin to as much as 300m locally within the STZ. Formed in shallow marine to paralic environments the Gassum Formation consists of interbedded fine- to medium-grained, occasionally coarse-grained and pebbly sandstones, heteroliths, mudstones and few thin coaly beds (Bertelsen 1978; Hamberg and Nielsen, 2000; Nielsen, 2003). The overlying Lower Jurassic (Hettangian–lowermost Aalenian) Fjerritlev Formation is dominated by marine claystones and mudstones. The transition from the Gassum to the Fjerritslev Formation occurred in several steps ranging from the latest Rhaetian in the central part of the basin to the Early Sinemurian along its northeastern margin, reflecting the overall Early Jurassic eustatic sea-level rise. Previous palynological studies of the Rhaetian-Hettangian in the Danish Basin and Scania have provided a biostratigraphic zonation for Rhaetian–Hettangian strata, as well as important information on depositional environment and palaeoclimate (Lund, 1977; Guy-Ohlson, 1981; Dybkjær, 1991; Koppelhus and Batten, 1996; Poulsen, 1996; Lindström and Erlström, 2006).

The Stenlille Structure

The Stenlille area (Figure DR1) is a very gentle anticlinal structure formed on top of a salt pillow and holds one of the most complete cored T/J boundary successions known, expanded in comparison to many other areas. Approximately 20 wells have been drilled through the Fjerritslev and Gassum Formations on the structure to assess the cap rock and reservoir quality, respectively, as the structure is used for storage of natural gas. The well-sections have been correlated by means of sedimentology and sequence stratigraphy, based on log-patterns, core interpretations, and biostratigraphic analyses (Hamberg and Nielsen, 2000; Nielsen, 2003). Based on the thick cored succession in the Stenlille-1 well supplemented with cores from the closely located Stenlille-2 and -3 wells a composite cored succession covering most of the Rhaetian–earliest Sinemurian is presented in this paper. The main part consists of one longer continuous and two short cored intervals from the Stenlille-1, complemented by two additional core sections from the Stenlille-2 and -5 (Figure DR2).

Within the Danish Basin the late Rhaetian maximum flooding event MFS7 (Nielsen, 2003) is a useful marker that is widely recognized all over the basin (based on log-patterns, sedimentology and biostratigraphy). In the more proximal parts of the basin it is recognized as a marine incursion in an otherwise predominantly terrestrial environment (Lindström and Erlström, 2006). The MSF7 can also be used for correlation outside the Danish Basin, e.g. in Germany where it appears to correspond roughly to the onset of the *Contorta*- Beds, while in St Audrie's Bay, Great Britain, it is correlated with the middle Westbury Formation (Lindström and Erlström 2006; Hounslow et al., 2004; Hesselbo et al., 2004). In the Danish well Rødby-1 in the North German Basin the base of the *Ogmoconchella aspinata* ostracod Zone and the typical Jurassic ammonite *Psiloceras planorbis* are located 2.4m and 13m above the MFS7, respectively (Nielsen, 2003).

Correlations within the Danish Basin are based primarily on palynostratigraphic events, and the most important are shown in Figures 2 and 3. One palynological marker that has gained increased interest in recent years is the first occurrence (FO) of *Cerebropollenites thiergartii,* which is now the accessory marker for the T/J boundary GSSP at Kuhjoch, Austria (Kürschner et al., 2007; Bonis et al., 2009; von Hillebrandt and Krystyn, 2009). However, at the base of its range *C. thiergartii* is generally represented only by very rare specimens, thus the exact level of its first appearance may be difficult to pinpoint.

METHODS

Sampling

A composite and almost fully cored section was built by combining good quality conventional cores from the Stenlille-1, -2 and -5 wells (Figures DR1, DR2). The wells are closely located within the same position in the basin and the depositional units can easily be correlated between the wells by means of the detailed well-log patterns (Figures DR1, DR2). Core depths were adjusted to log depths in their respective well by comparing core lithology to log interpretations. Hereafter the cores from Stenlille-2 and -5 were placed at the corresponding log patterns in the Stenlille-1 well so a well-constrained almost continuously cored composite section was established (Figure DR2). The depth intervals discussed below refer to the depths in the Stenlille-1 well. High-resolution sampling was carried out on the main cored succession of Stenlille-1 with generally 2–4 samples per meter across the boundary interval. The complementary cores were sampled with 1-3 samples per meter (Figure DR2).

Palynology

For palynology, ca 20 g of bulk rock was treated in alternating steps with hydrochloric (38%) and hydrofluoric acid (40%) to remove carbonate and silicate mineral phases. After washing to neutrality, residues were sieved with 11 µm mesh-size sieves and mounted on strew slides. Up to 300 palynomorphs were counted per slide with a compound microscope at 650x magnification. Abundance data were calculated as percentages of total palynomorph assemblage.

Geochemistry

One hundred and twenty-seven samples from the Stenlille cores were treated with HCl prior to carbon isotopic analysis to remove all carbonate. The residues were rinsed several times with distilled water, dried for 3 days at 80°C and subsequently ground to a homogeneous powder using an agate mortar. Depending on their TOC content sample aliquots of 3–10 mg were weighed and wrapped into tin capsules. At least two aliquots were prepared per sample. Carbon isotope analysis of TOC was subsequently performed using a Flash Elemental Analyzer 1112 (Thermoquest), connected to the continuous flow inlet system of a MAT gas source mass spectrometer (Thermoquest) at the Institute of Geosciences (Goethe University Frankfurt). USGS 24 standard was analyzed along with the samples in order to prove for accuracy and precision. Both samples and standards reproduced within ±0.2‰. Approximately 0.5 grams of an additional forty-two samples where analyzed by EA-IRMS at Iso-Analytical Laboratory in Cheshire, UK. The samples were decarbonized with 1M HCl to remove all carbonate, and the residues were washed twice with destilled water and subsequently dried at 60°C prior to isotope analysis.

The $\delta^{13}C_{org}$ values for the Stenlille succession are presented in Table DR1.

REFERENCES

Bertelsen, F., 1978: The Upper Triassic–Lower Jurassic Vinding and Gassum Formations of the Norwegian–Danish Basin: DGU Series B., v. 3, 26pp.

Bonis. N.R., Kürschner, W.M.and Krystyn, L., 2009: A detailed palynological study of the Triassic_Jurassic transition in key sections of the Eiberg Basin (Northern Calcareous Alps, Austria): Review of Palaeobotany and Palynology, v. 156, p. 376-400.

Dybkjær, K., 1991: Palynological zonation and palynofacies investigation of the Fjerritslev Formation (Lower Jurassic–basal Middle Jurassic) in the Danish Subbasin: DGU Series A., v. 30, 150pp.

Erlström, M., Thomas, S.A., Deeks, N. and Sivhed, U., 1997: Structure and tectonic evolution of the Tornquist Zone and adjacent sedimentary basins in Scania and the southern Baltic Sea area: Tectonophysics, v. 271, p. 191-215.

Guy-Ohlson, D., 1981: Rhaeto–Liassic palynostratigraphy of the Valhall Bore No. 1, Scania: GFF, v. 103, p. 233-248.

Hamberg, L. and Nielsen, L.H., 2000: Shingled, sharp-based shoreface sandstones: depositional response to stepwise forced regression in a shallow basin, Upper Triassic Gassum Formation, Denmark, *in* Hunt, D., Gawthorpe, R.L., eds., Sedimentary responses to forced regressions: Geological Society Special Publications, v. 172, p. 69-89.

Hesselbo, S.P., Robinson, S.A., and Surlyk, F., 2004, Sea-level changes and facies development across potential Triassic-Jurassic boundary horizons, SW Britain: Journal of the Geological Society, v. 161, p. 365–379.

Hounslow, M.W., Posen, P.E. and Warrington, G., 2004: Magnetostratigraphy and biostratigraphy of the Upper Triassic and lowermost Jurassic succession, St. Audrie's Bay, UK: Palaeogeography, Palaeoclimatology, Palaeoecology, v. 213, p. 331-358.

Kaufmann, A.J. and Xiao, S., 2003: High CO2 levels in the Proterozoic atmosphere estimated from analyses of individual microfossils: Nature, v. 425, p. 279-282.

Koppelhus, E.B. and Batten, D.J., 1996: 20C – Application of a palynomorph zonation to a series of short borehole sections, Lower to Middle Jurassic, Øresund, Denmark, *in* Jansonius, J. and McGregor, D.C., eds., Palynology: principles and applications: American Association of Stratigraphical Palynologists Foundation, v. 2, p. 779-793.

Kuerschner, W.M, Bonis, N.R. and Krystyn, L., 2007: Carbon-isotope stratigraphy and palynostratigraphy of the Triassic-Jurassic transition in the Tiefengraben section – Northern

Calcareous Alps (Austria): Palaeogeography, Palaeoclimatology, Palaeoecology, v. 244, p. 257-280.

Liboriussen, J., Ashton, P. and Tygesen, T., 1987: The tectonic evolution of the Fennoscandian Border Zone in Denmark, *in* Ziegler, P.A., ed., Compressional intra-plate deformations in the Alpine Foreland: Tectonophysics, v. 137, p. 21-29.

Lindström, S. and Erlström, M., 2006. The late Rhaetian transgression in southern Sweden: Regional (and global) recognition and relation to the Triassic-Jurassic boundary: Palaeogeography, Palaeoclimatology, Palaeoecology, v. 241, p. 339-372. doi:10.1016/j.palaeo.2006.04.006

Lund, J.J., 1977: Rhaetic to Lower Liassic palynology of the onshore south-eastern North Sea Basin: DGU II Række, v. 109, 129pp.

Michelsen, O., 1975: Lower Jurassic biostratigraphy and ostracods of the Danish Embayment: DGU II Række, v. 104, 287pp.

Michelsen, O., 1989: Revision of the Jurassic Lithostratigraphy of the Danish Subbasin: DGU Serie A, v. 24, 21pp.

Mogensen, T.E. and Korstgård, J.A., 2003: Triassic–Jurassic transtension along part of the Sorgenfrei-Tornquist Zone in the Danish Kattegat: Geological Survey of Denmark and Greenland Bulletin, v. 1, p. 439-458.

Nielsen, L.H., 2003, Late Triassic–Jurassic development of the Danish Basin and the Fennoscandian Border Zone, southern Scandinavia: Geological Survey of Denmark and Greenland Bulletin, v. 1, p. 459–526.

Pedersen, G., 1985: Thin, fine-grained storm layers in a muddy shelf sequence: an example from the Lower Jurassiv in the Stenlille 1 well, Denmark: Journal of the Geological Soviety of London, v. 142, p. 357-374.

Poulsen, N.E., 1996: Dinoflagellate cysts from marine Jurassic deposits of Denmark and Poland: American Association of Stratigraphical Palynolynologists, Contribution Series, v. 31, 227pp.

Tanner, L.H., Lucas, S.G. and Chapman, M.G. 2004: Assessing the record and causes of Late Triassic extinctions: Earth-Science Reviews 65, 103-139.

Vejbæk, O.V., 1989: Effects of asthenospheric heat flow in basin modelling exemplified with the Danish Basin: Earth and Planetary Science Letters, v. 95, p. 97-114.

von Hillebrandt, A. and Krystyn, L. 2009: On the oldest Jurassic ammonites of Europe (Northern Calcareous Alps, Austria) and their global significance: Neues Jahrbuch für Geologie und Paläontologie, Abhandlungen, v. 253, p. 163-195. DOI: 10.1127/0077-7749/2009/0253-0163

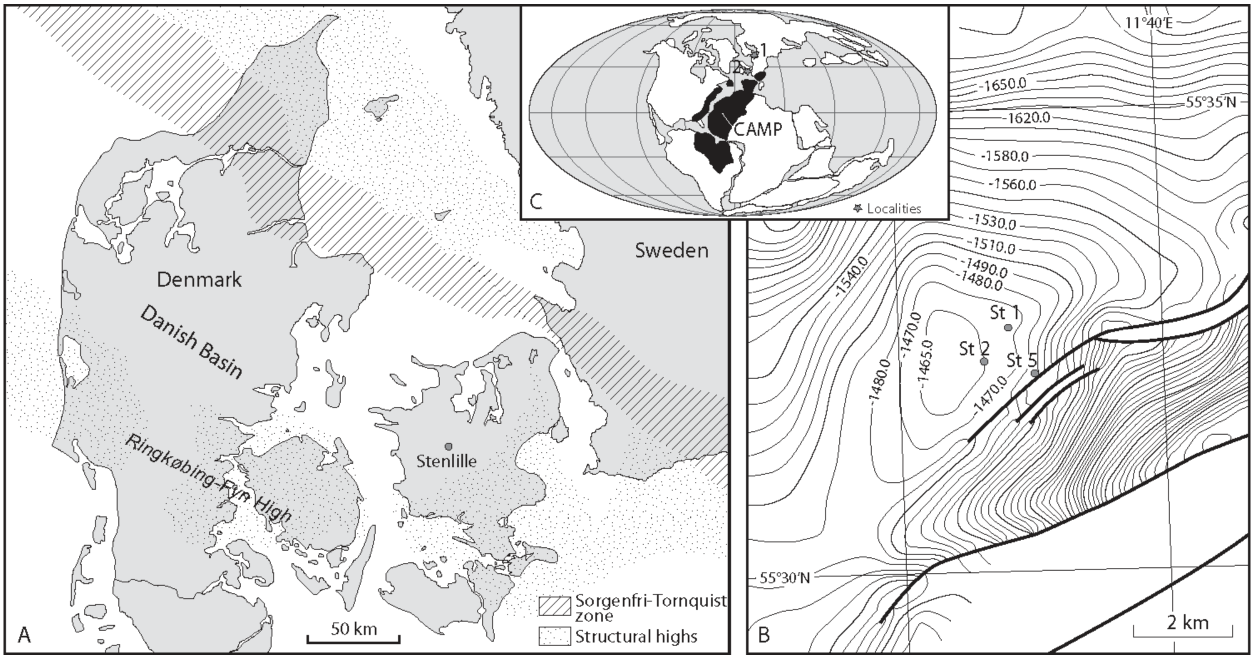

Data Repository Figure DR1. (A) Location of the Stenlille area, Denmark. (B) Isopach map over the Stenlille structure showing depth to top Gassum Formation and location of the three wells, Stenlille-1, -2 and –5 (St-1, St-2, St-5) included in this study. (C) Palaeogeographical map over Pangea (after Tanner et al. 2004) showing the extent of the Central Atlantic Magmatic Province, CAMP, and the location of the main localities discussed herein: 1. Stenlille, Danish Basin, 2. St Audrie's Bay and Doniford, UK.

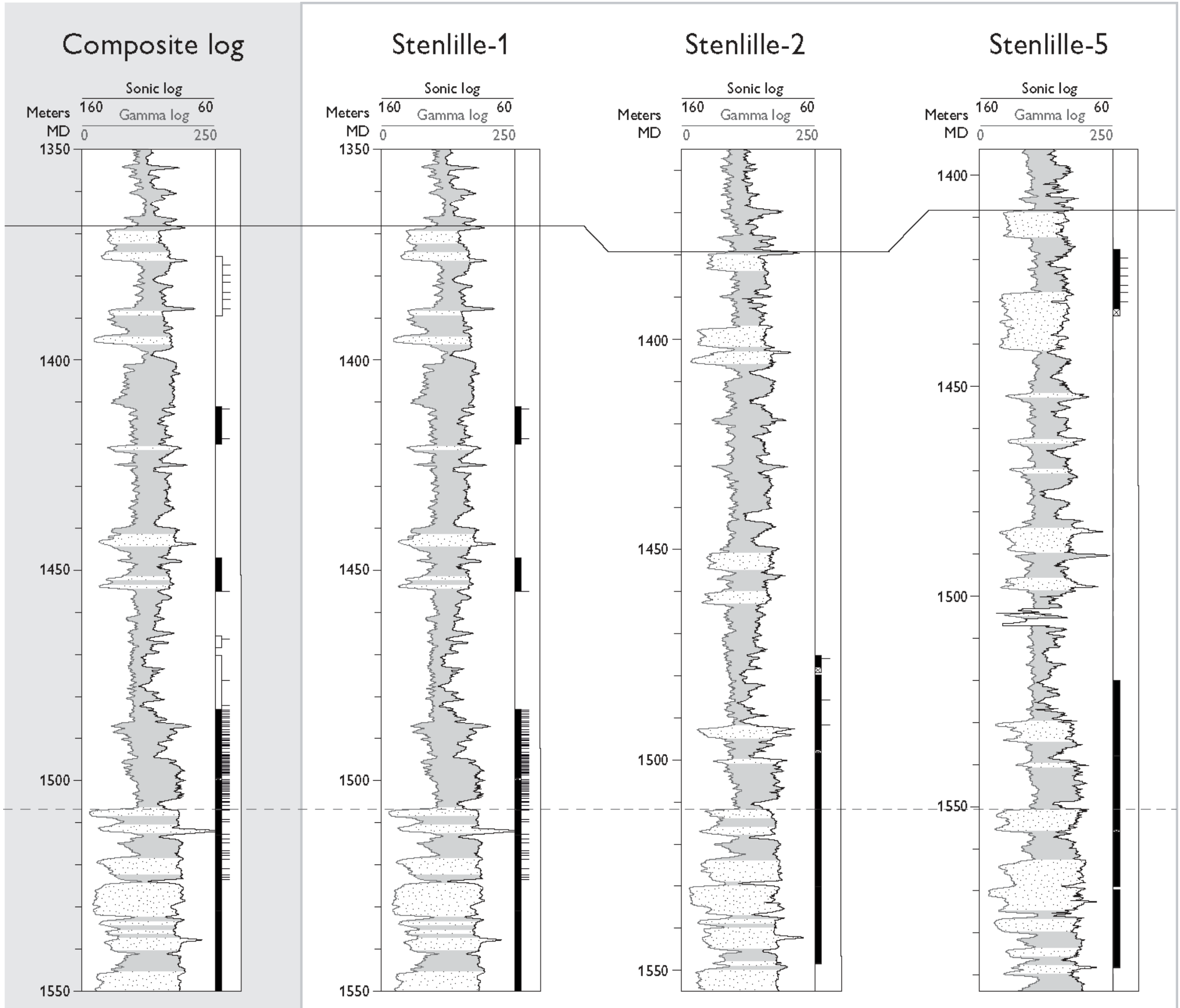

Data Repository Figure DR2. Correlation of the geophysical (gamma and sonic) logs and cored sections (in black) of the Stenlille-1, -2 and –5 wells. On the composite log on the left the corresponding position of the complementary cored intervals from Stenlille-2 and –5 are show in white.

Table DR1. δ^{13}C-org values for the Stenlille succession.

core	depth in core	δ13C
St-5	1419.86	-26.0
St-5	1421.03	-26.1
St-5	1421.53	-26.1
St-5	1422.15	-25.9
St-5	1422.54	-25.9
St-5	1423.33	-26.1
St-5	1423.95	-26.1
St-5	1424.99	-26.1
St-5	1425.60	-26.1
St-5	1426.15	-26.2
St-5	1426.89	-26.2
St-5	1427.20	-26.1
St-5	1427.91	-26.2
St-5	1428.44	-26.1
St-5	1428.94	-26.1
St-5	1430.08	-26.3
St-1	1411.90	-26.5
St-1	1413.38	-26.1
St-1	1414.38	-26.4
St-1	1415.28	-26.4
St-1	1416.04	-26.5
St-1	1416.89	-26.3
St-1	1418.18	-26.3
St-1	1418.95	-26.4
St-1	1447.73	-26.0
St-1	1448.46	-26.7
St-1	1450.16	-26.4
St-1	1451.06	-26.6
St-1	1451.67	-26.4
St-1	1453.21	-26.7
St-1	1455.02	-26.6
St-1	1455.12	-26.4

core	depth in core	δ13C
St-1	1483.25	-25.7
St-1	1483.55	-25.6
St-1	1485.08	-24.7
St-1	1485.88	-24.7
St-1	1486.60	-24.6
St-1	1487.26	-24.3
St-1	1487.72	-24.5
St-1	1488.22	-24.8
St-1	1488.55	-24.6
St-1	1489.05	-24.3
St-1	1489.57	-24.6
St-1	1489.57	-24.6
St-1	1489.90	-24.7
St-1	1490.50	-24.8
St-1	1490.50	-24.8
St-1	1491.01	-24.6
St-1	1491.77	-26.2
St-1	1492.43	-26.1
St-1	1492.82	-26.0
St-1	1492.82	-26.0
St-1	1493.25	-25.9
St-1	1493.63	-26.0
St-1	1494.00	-26.1
St-1	1494.17	-26.0
St-1	1494.31	-26.0
St-1	1494.44	-26.2
St-1	1494.60	-27.0
St-1	1494.64	-28.3
St-1	1494.73	-28.1
St-1	1494.90	-26.1
St-1	1494.90	-26.2
St-1	1495.03	-28.0
St-1	1495.10	**-26.6**
St-1	1495.10	**-26.6**
St-1	1495.51	-26.0

core	depth in core	δ13C
St-1	1498.57	-24.3
St-1	1498.72	-24.3
St-1	1498.72	-24.3
St-1	1499.56	-26.1
St-1	1499.79	-26.7
St-1	1500.07	-24.5
St-1	1500.07	-24.4
St-1	1500.44	-24.8
St-1	1500.70	-24.5
St-1	1500.70	-24.5
St-1	1501.00	-24.1
St-1	1501.80	-25.8
St-1	1502.24	-24.7
St-1	1502.24	-24.7
St-1	1502.62	-24.7
St-1	1503.10	-24.8
St-1	1503.10	-24.7
St-1	1503.35	-24.8
St-1	1503.70	-24.5
St-1	1503.70	-24.3
St-1	1504.21	-25.3
St-1	1504.91	-25.2
St-1	1504.91	-25.1
St-1	1505.23	-25.8
St-1	1505.81	-25.6
St-1	1506.02	-24.8
St-1	1506.02	-24.7
St-1	1506.41	-25.0
St-1	1506.41	-25.0
St-1	1506.57	-25.8
St-1	1506.57	-24.9
St-1	1506.82	-24.7
St-1	1506.82	-24.7
St-1	1507.08	-26.9
St-1	1507.10	-27.5

core	depth in core	δ13C
St-1	1512.99	-26.7
St-1	1513.53	-25.7
St-1	1513.53	-25.7
St-1	1513.76	-25.4
St-1	1514.61	-25.6
St-1	1514.81	-25.5
St-1	1515.37	-25.9
St-1	1515.37	-25.9
St-1	1515.84	-25.4
St-1	1516.61	-25.7
St-1	1517.16	-26.3
St-1	1517.77	-26.0
St-1	1518.22	-25.1
St-1	1518.74	-25.6
St-1	1519.29	-25.3
St-1	1519.29	-25.2
St-1	1519.64	-25.4
St-1	1520.08	-25.2
St-1	1520.19	**-26.2**
St-1	1520.19	**-25.0**
St-1	1521.27	-25.3
St-1	1521.91	-25.3
St-1	1522.44	-25.1
St-1	1522.89	-24.8
St-1	1523.46	-26.3
St-1	1523.46	-26.3

St-1 = Stenlille-1
St-2 = Stenlille-2
St-5 = Stenlille-5

St-2	1476.08	-26.3	St-1	1495.64	-25.1	St-1	1507.10	-27.3
St-2	1477.20	-26.3	St-1	1495.66	-24.5	St-1	1507.82	-25.4
St-2	1478.02	-26.5	St-1	1495.84	-24.3	St-1	1508.26	-26.4
St-2	1480.79	-26.8	St-1	1496.00	-24.6	St-1	1509.14	-26.1
St-2	1481.40	-26.7	St-1	1496.60	-24.9	St-1	1509.64	-25.7
St-2	1482.30	-26.9	St-1	1496.85	-25.1	St-1	1509.77	-25.7
St-2	1484.80	-26.8	St-1	1497.01	-25.0	St-1	1509.77	-25.7
St-2	1485.80	-26.9	St-1	1497.17	-26.2	St-1	1509.77	-25.6
St-2	1486.37	-27.1	St-1	1497.61	-23.9	St-1	1510.31	-25.8
St-2	1487.39	-26.5	St-1	1497.87	-24.8	St-1	1510.31	-25.8
St-2	1488.35	-25.8	St-1	1497.87	-24.8	St-1	1510.95	-25.5
St-2	1489.80	-25.7	St-1	1498.09	-24.3	St-1	1511.73	-25.8
St-2	1490.80	-26.3	St-1	1498.36	-24.2	St-1	1512.15	-26.4
St-2	1491.78	-26.1	St-1	1498.57	-24.4	St-1	1512.15	-26.0